JACS
JOURNAL OF THE AMERICAN CHEMICAL SOCIETY
pubs.acs.org/JACS
Communication

Synergistic Photoenzymatic Anti-Markovnikov Hydroarylation of Olefins via Heteroaryl Radical Intermediates

Prasun Mukherjee, Zayed Alassad, and Todd K. Hyster*

Cite This: https://doi.org/10.1021/jacs.5c01066
Read Online
ACCESS | Metrics & More | Article Recommendations | Supporting Information

ABSTRACT: Heteroaromatic alkylations are indispensable reactions for synthesizing biologically active molecules. The anti-Markovnikov hydroarylation of olefins using heteroaryl halides furnishes the product as a single regioisomer; however, catalytic variants are ineffective at controlling the stereochemical outcome of these reactions. Here, we report a synergistic photoenzymatic hydroarylation of olefins using flavin-dependent "ene"-reductases with ruthenium photoredox catalysts. Enzyme homologues were identified, which provide access to both product enantiomers in greater than 80% yield with up to 99:1 er. This method is effective for styrenyl- and unactivated alkenes, highlighting the generality of this approach. The highest yielding system involves a carboxylated photocatalyst with increased affinity for the enzyme. This work expands the types of radical intermediates that enzymes can use for stereoselective intermolecular coupling reactions.

Heteroaromatics are essential structural components of small-molecule pharmaceutical and agrochemical compounds (Figure 1a).[1] As the percentage of sp^3-hybridized atoms in drugs increases, there is an expanded need for pyridyl structures with adjacent stereocenters.[2,3] Benzylic and homobenzylic stereocenters are traditionally set via asymmetric reduction of the corresponding alkene.[4,5] While these methods offer unparalleled levels of enantioselectivity, they do not build molecular complexity. Transition-metal and Brønsted acid-catalyzed cross-couplings and conjugate additions to vinylpyridines also provide access to alkylated heterocycles; however, there remains a need for alternative asymmetric reactions that use readily available starting materials.[6−14]

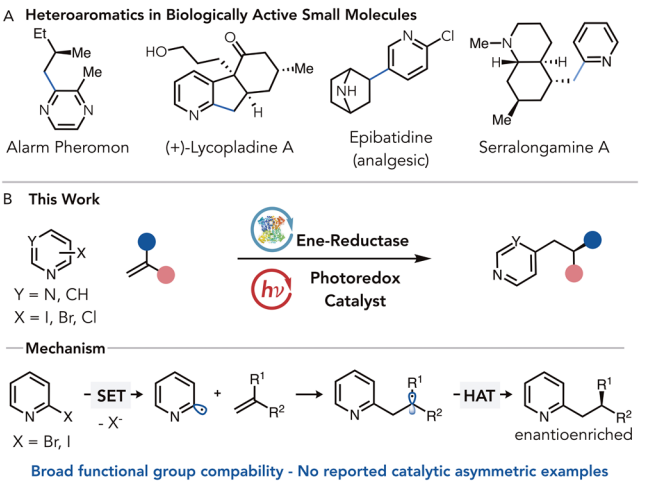

Figure 1. Synthesis of heteroaromatics with stereocenters. A) Examples of heteroaromatics in biologically active molecules. B) Olefin hydroarylation using aryl radicals. C) Synergistic photoenzymatic strategy for asymmetric hydroarylation.

Olefin hydroarylations are attractive for preparing structurally complex alkyl-substituted pyridines with benzylic and homobenzylic stereocenters. This general coupling reaction can be achieved using a few distinct catalytic strategies, including aromatic C−H activation,[15−17] reductive Heck reactions,[18] metal-catalyzed hydrogen atom transfer to olefins,[19−21] and reductive radical couplings using photoredox catalysts.[22−25] Despite the bevy of synthetic methods, none of these reactions have been rendered asymmetric.

Enzymes are ideal scaffolds for asymmetric synthesis because they can use numerous noncovalent interactions to control the reaction trajectories of highly reactive intermediates.[26] Over the past decade, our group has pioneered the area of photoenzymatic catalysis, where photonic energy is used to drive biocatalytic transformations.[27] Our group and others demonstrated that flavin-dependent "ene"-reductases (EREDs) could generate alkyl- and nitrogen-centered radicals for olefin hydroalkylation and hydroamination reactions.[28−43] Reactions occur with high levels of enantioselectivity because the protein can preferentially deliver a hydrogen atom to one prochiral face of the alkyl radical formed after C−C or C−N bond formation. Hydrogen atom transfer remains a challenging mechanistic step to render asymmetry, with reports only recently demonstrating the ability of small-molecule thiols to achieve this feat.[44,45]

Based on the ability of EREDs to control HAT, we questioned whether they could catalyze asymmetric hydroarylations using heteroaryl radicals (Figure 1b). Based on

Received: January 22, 2025
Revised: March 31, 2025
Accepted: April 10, 2025

Table 1. Reaction Optimization[a]

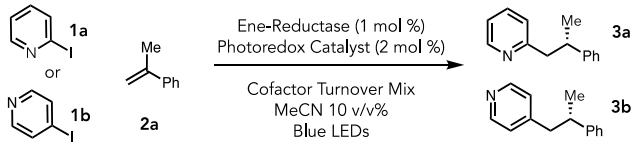

Entry	Product	ERED	Photocatalyst	Yield (%)	Enantiomeric Ratio (e.r.)
1[b]	**3a**	OYE3	-	1	98:2
2	**3a**	OYE3	$Ru(bpy)_3Cl_2$	25	96:4
3	**3a**	OYE3	$Ru(bpy)_2(4,4'\text{-}CO_2Hbpy)Cl_2$ (PC7)	54	96:4
4[c]	**3a**	GluER-T36A-Y177F	$Ru(bpy)_2(4\text{-}CO_2Hbpy)Cl_2$ (PC6)	25	3:97
5[d]	**3b**	OYE3	$Ru(bpy)_2(4\text{-}CO_2Hbpy)Cl_2$	78	97:3
6[e]	**3b**	OYE3	$Ru(bpy)_2(4\text{-}CO_2Hbpy)Cl_2$	59	96:4
7[f]	**3b**	OYE3	$Ru(bpy)_2(4\text{-}CO_2Hbpy)Cl_2$	29	91:9
8[g]	**3b**	OYE3	$Ru(bpy)_2(4\text{-}CO_2Hbpy)Cl_2$	41	97:3
9[h]	**3b**	OYE3	$Ru(bpy)_2(4\text{-}CO_2Hbpy)Cl_2$	36	97:3

[a]Reaction conditions: 2-iodopyridine **1a** (20 μmol), **2a** (5 equiv), $NADP^+$ (1 mol %), GDH-105 (1.5 mg), glucose (1 equiv), MES buffer (pH 6, 100 mM, 750 μL), acetonitrile (250 μL), blue LEDs, 17 h. [b]**2a** (3 equiv), GDH-105 (0.1 mg), glucose (1 equiv). [c]Glucose (2 equiv), acetonitrile (180 mL, 18% v/v). [d]4-Iodopyridine **1b** (20 μmol), **2a** (3 equiv), GDH-105 (0.1 mg), glucose (1 equiv). [e]OYE3 (0.5 mol %), 4-iodopyridine **1b** (20 μmol), **2a** (3 equiv), GDH-105 (0.1 mg). [f]OYE3 (0.1 mol %), 4-iodopyridine **1b** (20 μmol), [g]4-Bromopyridine was used instead of **1b**, **2a** (3 equiv), GDH-105 (0.1 mg). [h]4-Chloropyridine was used as a substrate instead of **1b**, **2a** (3 equiv), GSH-105 (0.1 mg).

pioneering studies by Jui, we hypothesized that aryl halides could be photochemically reduced to generate an aryl radical.[22−25] This ambiphilic intermediate can react with electronically diverse alkenes to afford an alkyl radical which is reductively quenched via HAT from the flavin cofactor.[46]

We began by exploring the coupling of 2-iodopyridine **1a** with α-methylstyrene using a series of ERED homologues in the presence of a cofactor turnover system to reduce the enzyme to the hydroquinone (FMN_{hq}) oxidation state while irradiating with blue LEDs (Table 1). While electron-deficient aryl halides are known to form charge transfer complexes with electron donors (amines, thiolates),[47−50] no product was formed under these conditions (Supporting Information Table 24, entry 2). We hypothesized that the lack of product formation was due to back electron transfer from the aryl radical anion to the flavin semiquinone (FMN_{sq}) being fast compared to mesolytic cleavage of the C−I bond.[51,52] To slow back electron transfer rates, we explore using exogenous photocatalysts for radical initiation. Previous studies found that exogenous photocatalysts could generate radicals when the biological cofactor alone was ineffective.[28,32,35,53,54] When catalytic quantities of $Ru(bpy)_3Cl_2$ were added to a reaction containing old yellow enzyme 3 (OYE3), the hydroarylated product was formed in 25% yield with 96:4 e.r. favoring the (*S*)-enantiomer (Table 1, entry 2). We hypothesized that superior yields could be achieved by modifying the photocatalyst structure. Adding two carboxylates to the 4,4′ positions of one of the bipyridine ligands increased the yield to 54% with no change in enantioselectivity (Table 1, entry 3). The (*R*)-enantiomer of the product can be formed in 29% yield using a previously identified variant of the ERED from *Gluconobacter oxidans* (GluER-T36A-Y177F) (Table 1, entry 4).

When exploring other iodopyridine isomers, we found that 4-iodopyridine was more reactive, affording the coupled product in 78% yield with 97:3 er when using $Ru(bpy)_2(4\text{-}CO_2Hbpy)$ as the photocatalyst (Table 1, entry 5). Lowering the enzyme loading to 0.5 and 0.1 mol % resulted in lower yields with a modest decrease in enantioselectivity (Table 1, entries 6 and 7). We were pleased that 4-bromo and 4-chloropyridines were effective radical precursors, producing 41 and 36% yields, respectively (Table 1, entries 8 and 9). Reactions can be run on a preparative scale using crude enzyme lysate, affording the product in 30% yield with 97:3 er, while reactions with purified enzyme formed the product in 60% yield with 97:3 er (Supporting Information Figures S2 and S3). We attribute lower yields to decreased photon flux due to lysate opacity.

We explored the alkene scope and limitations of the reaction using 4-iodopyridines as a radical precursor (Figure 2, **3b−3y**). We tested different substituted α-methylstyrenes and found that the enzyme tolerates varying electron-donating groups on

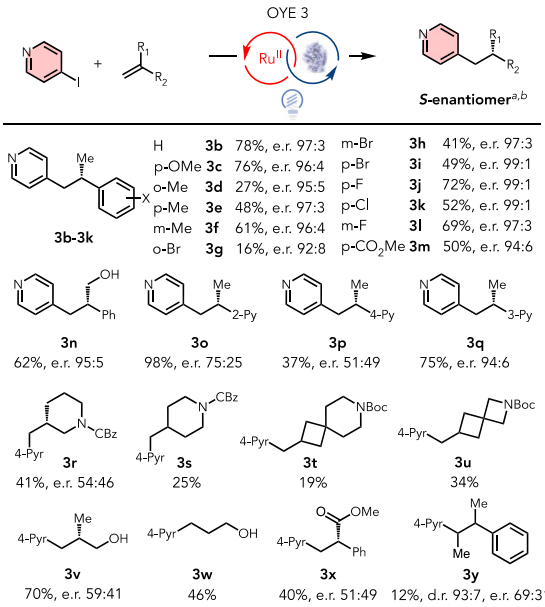

Figure 2. Scope of olefins. Reaction conditions for the (*S*)-enantiomers: aryl iodide (20 μmol, 1 equiv), olefins (60 μmol, 3 equiv), purified aliquots of the OYE 3 (200 nmol, 1 mol %), photocatalyst 6 (2 mol %), NADP+ (1 mol %), GDH-105 (0.1 mg), glucose (1 equiv), acetonitrile (250 μL, 25% v/v), and MES buffer (pH 6, 100 mM, 750 μL). The reaction mixture was stirred at 360 rpm and irradiated with blue LEDs for 17h.

https://doi.org/10.1021/jacs.5c01066
J. Am. Chem. Soc. XXXX, XXX, XXX−XXX

the arene (Figure 2, **3b**−**3f**). Halogen substituents are also tolerated on the alkene, affording the product in good yield with high enantioselectivity (Figure 2, **3g**−**3l**). While *ortho*-substitution affords product in diminished yield, the high enantioselectivity indicates that these substituents impact the C−C bond formation more than the radical termination event (Figure 2, **3d** and **3g**). The enzyme tolerates unprotected aromatic allylic alcohols, highlighting the functional group tolerance of the reaction (Figure 2, **3n**). Vinylpyridines were efficient coupling partners for this reaction, providing the product in up to 98% yield with excellent enantioselectivity (Figure 2, **3o**−**3q**). Importantly, this reaction also accepts nonstyrenyl substrates, significantly expanding the types of products that can be accessed using this method. Protected piperidines bearing exocyclic methylenes were reactive (Figure 2, **3r** and **3s**). Spirocyclic cyclobutanes were also reactive but afforded products with lower yields (Figure 2, **3t** and **3u**). Unprotected aliphatic allylic alcohols are tolerated, producing products in good yields but low levels of enantioselectivity (Figure 2, **3v** and **3w**). The system accepts α,β-unsaturated alkenes but forms the product as a racemate (Figure 2, entry **3x**). Finally, but-2-en-2-ylbenzene is a reactive coupling partner, affording a product with high diastereoselectivity and modest enantioselectivity (Figure 2, **3y**).

Next, we explore the scope and limitations of heteroaromatic halides (Figure 3, **3aa**−**3ar**). This reaction accepts a diverse range of substituted iodopyridines decorated with electron-donating and -withdrawing groups on the pyridine ring (Figure 3, **3aa**−**3aj**). Notably, the reaction accepts 2-, 3-, and 4-iodopyridines, forming the product in good yield and selectivity, suggesting that the locations of the basic nitrogen relative to the radical do not significantly impact the reaction. Beyond pyridines, the reaction also accommodates various iodoquinolines. While the yields are more modest, the enantioselectivity remains high (Figure 3, **3ak**−**3an**). 2-Bromoquinoline can also afford the corresponding product in modest yields and selectivities (Figure 3, **3am**). 2-Iodopyrazine and 2-bromopyrimidine are also reactive and provide the corresponding products in good yields and excellent enantioselectivity (Figure 3, **3ao** and **3ap**). Finally, electron-deficient nonheteroaromatic aryl iodide provided the products in moderate yield but with high enantioselectivity (Figure 3, **3aq** and **3ar**). As halopyridines have a similar reduction potential (between −1.85 and −2.29 V vs SCE) to that of 4-iodoacetophenone (−1.85 V vs SCE),[22] these results suggest that the reduction potential is a better predictor of reactivity than the presence of a basic nitrogen. Moreover, as the photocatalyst cannot facilitate this reaction without the protein (Supporting Information Table 24), we hypothesize that binding to the protein active site attenuates the reduction potential of the substrate. GluER-T36A can be used to access the opposite product enantiomer by using the same starting materials. In general, this enzyme is less efficient, affording the product in lower yields with more modest levels of enantioselectivity.

Next, we investigated the improved performance of the carboxylated photocatalysts compared to that of $Ru(bpy)_3$. We hypothesized that the difference was due to enhanced binding of the photocatalyst to the protein. We conducted steady-state and time-resolved fluorescence quenching experiments to probe this possibility and observed static quenching, indicating an association between the photocatalyst and OYE3. From these experiments, we measured a dissociation constant of K_d =

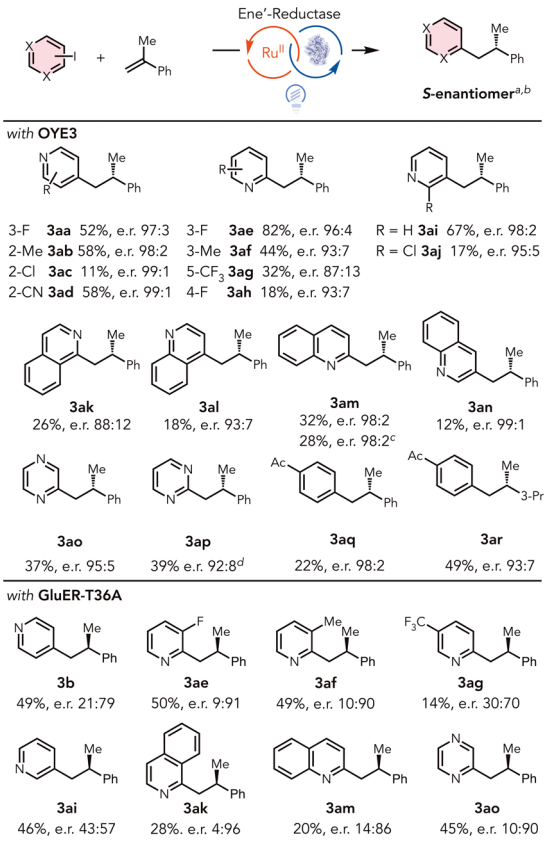

Figure 3. Scope of heterocycles. Reaction conditions for the (*S*)-enantiomers: aryl iodide (20 μmol, 1 equiv), olefins (60 μmol, 3 equiv), purified OYE 3 aliquot (200 nmol, 1 mol %), photocatalyst 6 (2 mol %), NADP+ (1 mol %), GDH-105 (0.1 mg), glucose (1 equiv), acetonitrile (250 μL, 25% v/v), MES buffer (pH 6, 100 mM, 750 μL). The reaction mixture was stirred at 360 rpm and irradiated with blue LEDs for 17 h. Photocatalyst 7 was used for entries **3ae**−**3ah**. Reaction conditions for the (*R*)- enantiomers: aryl iodide (20 μmol, 1 equiv), olefins (60 μmol, 3 equiv), purified GluER T36A aliquot (200 nmol, 1 mol %), photocatalyst 6 (2 mol %), NADP+ (1 mol %), GDH-105 (0.1 mg), glucose (2 equiv), acetonitrile (180 μL, 18% v/v), MES buffer (pH 6, 100 mM, 800 μL). The reaction mixture was stirred at 360 rpm and irradiated with blue LEDs for 17 h. [a]The yield (average of three runs) was determined using LCMS relative to internal standard 1,3,5-tribromobenzene. [b]e.r. was determined by using HPLC on a chiral stationary phase. [c]2-Bromoquinoline was used as a radical precursor. [d]2-Bromopyrimidine was used as a radical precursor.

6.7 nM for $Ru(bpy)_2(4,4'\text{-}CO_2Hbpy)$ while $Ru(bpy)_3$ has a higher value of K_d = 260 nM (Supporting Information Figures S18−S25).[28] As these two photocatalysts have similar reduction potentials ($Ru(bpy)_3^{II/I}$ = −1.175 V vs $Ru(bpy)_2(4,4'\text{-}CO_2Hbpy)^{II/I}$ = −1.25 V) (Supporting Information Figures S16 and S17), we hypothesize that stronger binding to the enzyme makes electron transfer between the photocatalyst and substrate, bound within the protein active site, more kinetically feasible.

While optimizing the reaction, we found that the formation of coupled product **3a** tracked closely with the consumption of 2-iodopyridine, indicating that hydrodehalogenation of the aryl halide is not favored under the reaction conditions (Figure 4a). Given the short lifetimes of aryl radicals, this observation suggests that both the alkene and aryl halide are bound within the protein active site prior to radical formation. To determine

https://doi.org/10.1021/jacs.5c01066
J. Am. Chem. Soc. XXXX, XXX, XXX−XXX

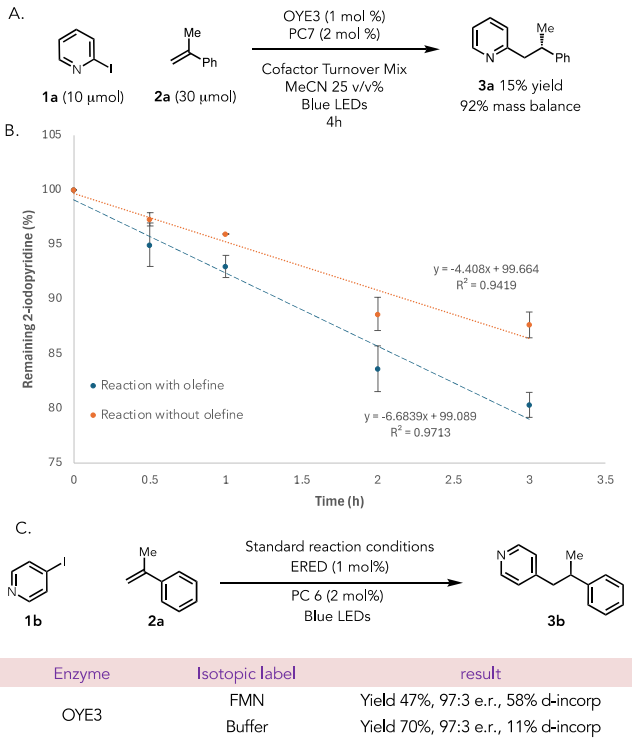

Enzyme	Isotopic label	result
OYE3	FMN	Yield 47%, 97:3 e.r., 58% d-incorp
	Buffer	Yield 70%, 97:3 e.r., 11% d-incorp

Figure 4. A) Formation of **3a** after 4 h. B) Kinetics of 2-iodopyridine consumption with and without alkene. C) Deuterium incorporation study.

whether the presence of an alkene accelerates the consumption of aryl halides, we explore the kinetics of the reaction with and without an alkene (Supporting Information Figure S4). During the initial rate of the reaction, we found that 2-iodopyridine is consumed 1.6 times faster in the presence of alkene than in its absence, indicating that the alkene is influencing the radical initiation event (Figure 4b).[55]

Finally, we conducted isotope incorporation experiments to determine the mechanism of radical termination (Supporting Information Figures S5–S13 and Figure 4c). When using 4-iodopyridine with D-glucose-1-d_1 to isotopically label the N5-position of the flavin cofactor, the product is isolated with 58% deuterium incorporation (Figure 4c). In contrast, when a buffer made with D_2O is used to isotopically label the O–H bonds of tyrosine phenols, we observe 11% deuterium incorporation. These results suggest that flavin is terminating the reaction via hydrogen atom transfer from flavin. Moderate levels of deuterium incorporation when using N5-labeled flavin hydroquinone are presumably due to redox cycling the flavin cofactor by the photoredox catalyst, leading to label exchange with buffer.

In conclusion, we have developed a photoenzymatic system to catalyze an asymmetric hydroarylation of alkenes using aryl halides as radical precursors. This work expands the types of reactive intermediates that EREDs can use for alkene functionalization. We expect this reactivity mode to be compatible with other photoenzymes for other non-natural catalytic functions.

■ ASSOCIATED CONTENT

Supporting Information

The Supporting Information is available free of charge at https://pubs.acs.org/doi/10.1021/jacs.5c01066.

Experimental procedures, characterization data, NMR spectra, and HPLC traces (PDF)

■ AUTHOR INFORMATION

Corresponding Author

Todd K. Hyster – *Department of Chemistry, Princeton University, Princeton, New Jersey 08544, United States;* orcid.org/0000-0003-3560-355X; Email: thyster@princeton.edu

Authors

Prasun Mukherjee – *Department of Chemistry, Princeton University, Princeton, New Jersey 08544, United States*

Zayed Alassad – *Department of Chemistry, Princeton University, Princeton, New Jersey 08544, United States*

Complete contact information is available at: https://pubs.acs.org/10.1021/jacs.5c01066

Notes

The authors declare no competing financial interest.

■ ACKNOWLEDGMENTS

The research reported here was supported by the National Science Foundation (CHE-2135973). The authors would like to acknowledge Venu Vandavasi for assistance running fluorescence quenching experiments.

■ REFERENCES

(1) Vitaku, E.; Smith, D. T.; Njardarson, J. T. Analysis of the Structural Diversity, Substitution Patterns, and Frequency of Nitrogen Heterocycles among U.S. FDA Approved Pharmaceuticals. *J. Med. Chem.* **2014**, *57* (24), 10257–10274.

(2) Lovering, F.; Bikker, J.; Humblet, C. Escape from Flatland: Increasing Saturation as an Approach to Improving Clinical Success. *J. Med. Chem.* **2009**, *52* (21), 6752–6756.

(3) Krzyzanowski, A.; Pahl, A.; Grigalunas, M.; Waldmann, H. Spacial Score-A Comprehensive Topological Indicator for Small-Molecule Complexity. *J. Med. Chem.* **2023**, *66*, 12739.

(4) Verendel, J. J.; Pàmies, O.; Diéguez, M.; Andersson, P. G. Asymmetric Hydrogenation of Olefins Using Chiral Crabtree-Type Catalysts: Scope and Limitations. *Chem. Rev.* **2014**, *114* (4), 2130–2169.

(5) Roseblade, S. J.; Pfaltz, A. Iridium-Catalyzed Asymmetric Hydrogenation of Olefins. *Acc. Chem. Res.* **2007**, *40* (12), 1402–1411.

(6) Pattison, G.; Piraux, G.; Lam, H. W. Enantioselective Rhodium-Catalyzed Addition of Arylboronic Acids to Alkenylheteroarenes. *J. Am. Chem. Soc.* **2010**, *132* (41), 14373–14375.

(7) Jumde, R. P.; Lanza, F.; Pellegrini, T.; Harutyunyan, S. R. Highly Enantioselective Catalytic Synthesis of Chiral Pyridines. *Nat. Commun.* **2017**, *8* (1), 2058.

(8) Jumde, R. P.; Lanza, F.; Veenstra, M. J.; Harutyunyan, S. R. Catalytic Asymmetric Addition of Grignard Reagents to Alkenyl-Substituted Aromatic N-Heterocycles. *Science* **2016**, *352* (6284), 433–437.

(9) Yang, J.-S.; Lu, K.; Li, C.-X.; Zhao, Z.-H.; Zhang, F.-M.; Zhang, X.-M.; Tu, Y.-Q. NiH-Catalyzed Regio- and Enantioselective Hydroalkylation for the Synthesis of β- or Γ-Branched Chiral Aromatic N-Heterocycles. *J. Am. Chem. Soc.* **2023**, *145* (40), 22122–22134.

(10) Appella, D. H.; Moritani, Y.; Shintani, R.; Ferreira, E. M.; Buchwald, S. L. Asymmetric Conjugate Reduction of α,β-Unsaturated Esters Using a Chiral Phosphine-Copper Catalyst. *J. Am. Chem. Soc.* **1999**, *121* (40), 9473–9474.

(11) Kong, M.; Tan, Y.; Zhao, X.; Qiao, B.; Tan, C.-H.; Cao, S.; Jiang, Z. Catalytic Reductive Cross Coupling and Enantioselective

Protonation of Olefins to Construct Remote Stereocenters for Azaarenes. *J. Am. Chem. Soc.* **2021**, *143* (10), 4024−4031.
(12) Fu, Q.; Cao, S.; Wang, J.; Lv, X.; Wang, H.; Zhao, X.; Jiang, Z. Enantioselective [2π + 2σ] Cycloadditions of Bicyclo[1.1.0]Butanes with Vinylazaarenes through Asymmetric Photoredox Catalysis. *J. Am. Chem. Soc.* **2024**, *146* (12), 8372−8380.
(13) Li, Y.; Han, C.; Wang, Y.; Huang, X.; Zhao, X.; Qiao, B.; Jiang, Z. Catalytic Asymmetric Reductive Azaarylation of Olefins via Enantioselective Radical Coupling. *J. Am. Chem. Soc.* **2022**, *144* (17), 7805−7814.
(14) Guo, J.; Xie, Y.; Lai, Z.-M.; Weng, J.; Chan, A. S. C.; Lu, G. Enantioselective Hydroalkylation of Alkenylpyridines Enabled by Merging Photoactive Electron Donor-Acceptor Complexes with Chiral Bifunctional Organocatalysis. *ACS Catal.* **2022**, *12* (20), 13065−13074.
(15) Zhang, W.-B.; Yang, X.-T.; Ma, J.-B.; Su, Z.-M.; Shi, S.-L. Regio- and Enantioselective C-H Cyclization of Pyridines with Alkenes Enabled by a Nickel/N-Heterocyclic Carbene Catalysis. *J. Am. Chem. Soc.* **2019**, *141* (14), 5628−5634.
(16) Lewis, J. C.; Bergman, R. G.; Ellman, J. A. Rh(I)-Catalyzed Alkylation of Quinolines and Pyridines via C-H Bond Activation. *J. Am. Chem. Soc.* **2007**, *129* (17), 5332−5333.
(17) Nakao, Y.; Yamada, Y.; Kashihara, N.; Hiyama, T. Selective C-4 Alkylation of Pyridine by Nickel/Lewis Acid Catalysis. *J. Am. Chem. Soc.* **2010**, *132* (39), 13666−13668.
(18) Gurak, J. A.; Engle, K. M. Practical Intermolecular Hydroarylation of Diverse Alkenes via Reductive Heck Coupling. *ACS Catal.* **2018**, *8* (10), 8987−8992.
(19) Liu, H.-C.; Xu, X.-Y.; Tang, S.; Bao, J.; Wang, Y.-Z.; Chen, Y.; Han, X.; Liang, Y.-M.; Zhang, K. Photoinduced Co/Ni-Cocatalyzed Markovnikov Hydroarylation of Unactivated Olefins with Aryl Bromides. *Chem. Sci.* **2024**, *15* (36), 14865−14871.
(20) Green, S. A.; Vásquez-Céspedes, S.; Shenvi, R. A. Iron-Nickel Dual-Catalysis: A New Engine for Olefin Functionalization and the Formation of Quaternary Centers. *J. Am. Chem. Soc.* **2018**, *140* (36), 11317−11324.
(21) Green, S. A.; Matos, J. L. M.; Yagi, A.; Shenvi, R. A. Branch-Selective Hydroarylation: Iodoarene-Olefin Cross-Coupling. *J. Am. Chem. Soc.* **2016**, *138* (39), 12779−12782.
(22) Boyington, A. J.; Seath, C. P.; Zearfoss, A. M.; Xu, Z.; Jui, N. T. Catalytic Strategy for Regioselective Arylethylamine Synthesis. *J. Am. Chem. Soc.* **2019**, *141* (9), 4147−4153.
(23) Seath, C. P.; Vogt, D. B.; Xu, Z.; Boyington, A. J.; Jui, N. T. Radical Hydroarylation of Functionalized Olefins and Mechanistic Investigation of Photocatalytic Pyridyl Radical Reactions. *J. Am. Chem. Soc.* **2018**, *140* (45), 15525−15534.
(24) Maust, M. C.; Hendy, C. M.; Jui, N. T.; Blakey, S. B. Switchable Regioselective 6-Endo or 5-Exo Radical Cyclization via Photoredox Catalysis. *J. Am. Chem. Soc.* **2022**, *144* (9), 3776−3781.
(25) Boyington, A. J.; Riu, M.-L. Y.; Jui, N. T. Anti-Markovnikov Hydroarylation of Unactivated Olefins via Pyridyl Radical Intermediates. *J. Am. Chem. Soc.* **2017**, *139* (19), 6582−6585.
(26) Cossy, J. Biocatalysts: Catalysts of the Future for Organic Synthesis and Beyond? *Tetrahedron* **2022**, *123*, 132966.
(27) Fu, H.; Hyster, T. K. From Ground-State to Excited-State Activation Modes: Flavin-Dependent "Ene"-Reductases Catalyzed Non-Natural Radical Reactions. *Acc. Chem. Res.* **2024**, *57* (9), 1446−1457.
(28) Sun, S.-Z.; Nicholls, B. T.; Bain, D.; Qiao, T.; Page, C. G.; Musser, A. J.; Hyster, T. K. Enantioselective Decarboxylative Alkylation Using Synergistic Photoenzymatic Catalysis. *Nat. Catal.* **2024**, *7* (1), 35−42.
(29) Bender, S. G.; Hyster, T. K. Pyridylmethyl Radicals for Enantioselective Alkene Hydroalkylation Using "Ene"-Reductases. *ACS Catal.* **2023**, *13* (22), 14680−14684.
(30) Fu, H.; Lam, H.; Emmanuel, M. A.; Kim, J. H.; Sandoval, B. A.; Hyster, T. K. Ground-State Electron Transfer as an Initiation Mechanism for Biocatalytic C-C Bond Forming Reactions. *J. Am. Chem. Soc.* **2021**, *143* (25), 9622−9629.
(31) Laguerre, N.; Riehl, P. S.; Oblinsky, D. G.; Emmanuel, M. A.; Black, M. J.; Scholes, G. D.; Hyster, T. K. Radical Termination via B-Scission Enables Photoenzymatic Allylic Alkylation Using "Ene"-Reductases. *ACS Catal.* **2022**, *12* (15), 9801−9805.
(32) Nakano, Y.; Black, M. J.; Meichan, A. J.; Sandoval, B. A.; Chung, M. M.; Biegasiewicz, K. F.; Zhu, T.; Hyster, T. K. Photoenzymatic Hydrogenation of Heteroaromatic Olefins Using 'Ene'-Reductases with Photoredox Catalysts. *Angew. Chem., Int. Ed.* **2020**, *59* (26), 10484−10488.
(33) Biegasiewicz, K. F.; Cooper, S. J.; Gao, X.; Oblinsky, D. G.; Kim, J. H.; Garfinkle, S. E.; Joyce, L. A.; Sandoval, B. A.; Scholes, G. D.; Hyster, T. K. Photoexcitation of Flavoenzymes Enables a Stereoselective Radical Cyclization. *Science* **2019**, *364* (6446), 1166−1169.
(34) Page, C. G.; Cooper, S. J.; DeHovitz, J. S.; Oblinsky, D. G.; Biegasiewicz, K. F.; Antropow, A. H.; Armbrust, K. W.; Ellis, J. M.; Hamann, L. G.; Horn, E. J.; Oberg, K. M.; Scholes, G. D.; Hyster, T. K. Quaternary Charge-Transfer Complex Enables Photoenzymatic Intermolecular Hydroalkylation of Olefins. *J. Am. Chem. Soc.* **2021**, *143* (1), 97−102.
(35) Ye, Y.; Cao, J.; Oblinsky, D. G.; Verma, D.; Prier, C. K.; Scholes, G. D.; Hyster, T. K. Using Enzymes to Tame Nitrogen-Centred Radicals for Enantioselective Hydroamination. *Nat. Chem.* **2023**, *15* (2), 206−212.
(36) Fu, H.; Cao, J.; Qiao, T.; Qi, Y.; Charnock, S. J.; Garfinkle, S.; Hyster, T. K. An Asymmetric Sp3-Sp3 Cross-Electrophile Coupling Using 'Ene'-Reductases. *Nature* **2022**, *610* (7931), 302−307.
(37) Huang, X.; Wang, B.; Wang, Y.; Jiang, G.; Feng, J.; Zhao, H. Photoenzymatic Enantioselective Intermolecular Radical Hydroalkylation. *Nature* **2020**, *584* (7819), 69−74.
(38) Zhang, Z.; Feng, J.; Yang, C.; Cui, H.; Harrison, W.; Zhong, D.; Wang, B.; Zhao, H. Photoenzymatic Enantioselective Intermolecular Radical Hydroamination. *Nat. Catal.* **2023**, *6* (8), 687−694.
(39) Harrison, W.; Jiang, G.; Zhang, Z.; Li, M.; Chen, H.; Zhao, H. Photoenzymatic Asymmetric Hydroamination for Chiral Alkyl Amine Synthesis. *J. Am. Chem. Soc.* **2024**, *146* (15), 10716−10722.
(40) Li, M.; Yuan, Y.; Harrison, W.; Zhang, Z.; Zhao, H. Asymmetric Photoenzymatic Incorporation of Fluorinated Motifs into Olefins. *Science* **2024**, *385* (6707), 416−421.
(41) Shi, Q.; Kang, X.-W.; Liu, Z.; Sakthivel, P.; Aman, H.; Chang, R.; Yan, X.; Pang, Y.; Dai, S.; Ding, B.; Ye, J. Single-Electron Oxidation-Initiated Enantioselective Hydrosulfonylation of Olefins Enabled by Photoenzymatic Catalysis. *J. Am. Chem. Soc.* **2024**, *146* (4), 2748−2756.
(42) Zhao, B.; Feng, J.; Yu, L.; Xing, Z.; Chen, B.; Liu, A.; Liu, F.; Shi, F.; Zhao, Y.; Tian, C.; Wang, B.; Huang, X. Direct Visible-Light-Excited Flavoproteins for Redox-Neutral Asymmetric Radical Hydroarylation. *Nat. Catal.* **2023**, *6* (11), 996−1004.
(43) Xing, Z.; Liu, F.; Feng, J.; Yu, L.; Wu, Z.; Zhao, B.; Chen, B.; Ping, H.; Xu, Y.; Liu, A.; Zhao, Y.; Wang, C.; Wang, B.; Huang, X. Synergistic Photobiocatalysis for Enantioselective Triple Radical Sorting. *Nature* **2025**, *637*, 1118−1123.
(44) Shin, N. Y.; Ryss, J. M.; Zhang, X.; Miller, S. J.; Knowles, R. R. Light - Driven Deracemization Enabled by Excited - State Electron Transfer. *Science* **2019**, *366* (6463), 364−369.
(45) Hejna, B. G.; Ganley, J. M.; Shao, H.; Tian, H.; Ellefsen, J. D.; Fastuca, N. J.; Houk, K. N.; Miller, S. J.; Knowles, R. R. Catalytic Asymmetric Hydrogen Atom Transfer: Enantioselective Hydroamination of Alkenes. *J. Am. Chem. Soc.* **2023**, *145* (29), 16118−16129.
(46) Parsaee, F.; Senarathna, M. C.; Kannangara, P. B.; Alexander, S. N.; Arche, P. D. E.; Welin, E. R. Radical Philicity and Its Role in Selective Organic Transformations. *Nat. Rev. Chem.* **2021**, *5* (7), 486−499.
(47) Pan, P.; Liu, S.; Lan, Y.; Zeng, H.; Li, C.-J. Visible-Light-Induced Cross-Coupling of Aryl Iodides with Hydrazones via an EDA-Complex. *Chem. Sci.* **2022**, *13* (24), 7165−7171.
(48) Zhao, H.; Cuomo, V. D.; Rossi-Ashton, J. A.; Procter, D. J. Aryl Sulfonium Salt Electron Donor-Acceptor Complexes for Halogen

https://doi.org/10.1021/jacs.5c01066
J. Am. Chem. Soc. XXXX, XXX, XXX−XXX

Atom Transfer: Isocyanides as Tunable Coupling Partners. *Chem.* **2024**, *10* (4), 1240−1251.
(49) Liang, K.; Li, N.; Zhang, Y.; Li, T.; Xia, C. Transition-Metal-Free α-Arylation of Oxindoles vi a Visible-Light-Promoted Electron Transfer. *Chem. Sci.* **2019**, *10* (10), 3049−3053.
(50) Liu, B.; Lim, C.-H.; Miyake, G. M. Visible-Light-Promoted C-S Cross-Coupling via Intermolecular Charge Transfer. *J. Am. Chem. Soc.* **2017**, *139* (39), 13616−13619.
(51) Andrieux, C. P.; Savéant, J.-M.; Tallec, A.; Tardivel, R.; Tardy, C. Concerted and Stepwise Dissociative Electron Transfers. Oxidability of the Leaving Group and Strength of the Breaking Bond as Mechanism and Reactivity Governing Factors Illustrated by the Electrochemical Reduction of α-Substituted Acetophenones. *J. Am. Chem. Soc.* **1997**, *119* (10), 2420−2429.
(52) Costentin, C.; Robert, M.; Savéant, J.-M. Fragmentation of Aryl Halide π Anion Radicals. Bending of the Cleaving Bond and Activation vs Driving Force Relationships. *J. Am. Chem. Soc.* **2004**, *126* (49), 16051−16057.
(53) Sandoval, B. A.; Kurtoic, S. I.; Chung, M. M.; Biegasiewicz, K. F.; Hyster, T. K. Photoenzymatic Catalysis Enables Radical-Mediated Ketone Reduction in Ene-Reductases. *Angew. Chem., Int. Ed.* **2019**, *58* (26), 8714−8718.
(54) Biegasiewicz, K. F.; Cooper, S. J.; Emmanuel, M. A.; Miller, D. C.; Hyster, T. K. Catalytic Promiscuity Enabled by Photoredox Catalysis in Nicotinamide-Dependent Oxidoreductases. *Nat. Chem.* **2018**, *10* (7), 770−775.
(55) Fu, H.; Lam, H.; Emmanuel, M.; Kim, J. H.; Sandoval, B.; Hyster, T. K. Ground-State Electron Transfer as an Initiation Mechanism for Asymmetric Hydroalkylations in Radical Biocatalysis. *J. Am. Chem. Soc.* **2021**, *143* (25), 9622−9629.

https://doi.org/10.1021/jacs.5c01066
J. Am. Chem. Soc. XXXX, XXX, XXX−XXX